A process-based *Sphagnum* plant-functional-type model for implementation in the TRIFFID Dynamic Global Vegetation Model

Richard Coppell[1], Emanuel Gloor[1], Joseph Holden[1]

[1]water@leeds, School of Geography, University of Leeds, Leeds, LS2 9JT, UK

5 *Correspondence to*: Richard Coppell (r.coppell@leeds.ac.uk)

Abstract. Peatlands are important carbon stores and *Sphagnum* moss represents a critical peatland genus contributing to carbon exchange and storage. However, gas fluxes in *Sphagnum*-dominated systems are poorly represented in Dynamic Global Vegetation Models (DGVMs) which simulate, via incorporation of Plant Functional Types (PFTs), biogeochemical and energy fluxes between vegetation, the land surface and the atmosphere. Mechanisms characterised by PFTs within DGVMs include

10 photosynthesis, respiration and competition and, in more recent DGVMs, sub-daily gas-exchange processes regulated by leaf stomata. However, *Sphagnum*, like all mosses, are non-vascular plants and do not exhibit stomatal regulation. In order to achieve a level of process detail consistent with existing vascular vegetation PFTs within DGVMs, this paper describes a new process-based non-vascular-PFT model that is implemented within the TRIFFID DGVM used by the JULES land surface model. The new PFT model was tested against extant published field and laboratory studies of peat assemblage-net primary

15 productivity, assemblage-gross primary productivity, assemblage respiration, water-table position, incoming photosynthetically active radiation, temperature, and canopy dark respiration. The PFT model's parameters were roughly tuned and the PFT model easily produced curves of the correct shape for peat assemblage-net primary productivity against water-table position, incoming photosynthetically active radiation and temperature, suggesting that it replicates the internal productivity mechanism of *Sphagnum* for the first time. Minor modifications should also allow it to be used across a range of

20 other bryophytes enabling this non-vascular PFT model to have enhanced functionality.

1 Introduction

Around 600Gt of carbon exists in peat that has accumulated in temperate and cold biomes since the Last Glacial Maximum (Yu et al. 2010, Yu 2011). This is about 25% of the carbon stored in deep soils (Jobaggy & Jackson 2000). Peat accumulates in areas where precipitation exceeds evapotranspiration and there is impeded drainage due to the landscape configuration or

25 underlying impermeable layers. There is uncertainty about feedback mechanisms between peatland systems and future climate change. For example, warming may enhance decomposition rates of peat and thus release of carbon to the atmosphere, but it may also enhance net primary production (NPP) and thus mitigate anthropogenic greenhouse warming (Loisel et al. 2012; Charman et al. 2013; O'Connor et al. 2010). This means that the net result on greenhouse gas fluxes regionally and globally is not clear and there is therefore a need for improved climate-land surface feedback models that incorporate such peatland

30 processes (Limpens et al. 2008; Frolking et al. 2009; Hayman et al. 2014).

Dynamic Global Vegetation Models (DGVMs) simulate carbon, water and energy fluxes between vegetation, the atmosphere and the land surface (e.g. Clark et al. 2011; Haxeltine & Prentice, 1996; Sitch et al. 2003). DGVMs may be run independently with prescribed climate or they can be coupled to climate models. For example, the TRIFFID DGVM is a sub-model of the

5   JULES land surface model which is in turn part of the Hadley Centre climate model (Clark et al. 2011; Pope et al. 2000). As such, DGVMs could be used in understanding past and future change in peatlands and their interactions with global climate. DGVMs simulate the effects of a limited number of vegetation classes (rather than every single species) in each horizontal grid square of the model, reflecting the assumption that regional vegetation assemblages are dominated by a small number of Plant Functional Types (PFTs) (Brovkin et al. 1997; Haxeltine & Prentice, 1996). The main vegetation processes represented

10   in DGVMs include photosynthesis and accumulation of atmospheric carbon in plant tissues, respiration, the accumulation of litter from dead plant material and plant competition. Therefore, for use in peatlands, DGVMs require appropriate incorporation of dominant peatland PFTs, and their associated relevant carbon exchange and litter accumulation processes.

In the current generation of DGVMs, vegetation-atmosphere CO_2 exchange is commonly represented at sub-daily time-steps,

15   incorporating regulation of gas exchange in vascular plants by leaf stomata that close in response to moisture deficit in the leaf (e.g. Cox, et al. 1998; Clark et al. 2011; Gao et al. 2013). *Sphagnum* mosses are a dominant genus within peatlands. At least half of the carbon in northern peatlands is dead matter from *Sphagnum* (Clymo & Hayward, 1982). However, there is a key problem with incorporating *Sphagnum* into DGVMs: *Sphagnum* is a non-vascular plant that lacks stomatal gas-exchange. Therefore, *Sphagnum* mosses show quite different responses of photosynthesis and respiration to changes in their immediate

20   environment compared to vascular plants and this means they cannot be simply incorporated into current DGVMs. For example, Riutta et al. (2007) examined gross primary production (GPP) of *Sphagnum* compared to vascular wetland plants, for different environmental conditions. Unlike vascular wetland plants, *Sphagnum* GPP showed a high tolerance to waterlogging, and little short-term temperature-dependence with much higher rates of production for temperatures below 20ºC than vascular wetland plants.

25

Sphagnum also causes changes in the local physical and chemical environment, slowing the rate of decay (Rydin et al 2006). *Sphagnum* cell walls and litter contain insoluble polysaccharides that inhibit microbial mineralisation, while the release of uronic acids from *Sphagnum* acidifies the soil water and hinders the decay of adjacent litter from other plants (Hájek et al. 2010; Van Breemen 1995). Thus, *Sphagnum* is associated with high rates of plant litter accumulation in cool, wet areas

30   resulting in peatland extents and depths that are larger than they would be without *Sphagnum* (Rydin & Jeglum, 2006).

Given the importance of *Sphagnum* to peatland systems and the global carbon store, it is essential that *Sphagnum* is appropriately incorporated into the latest-generation DGVMs. Variations do exist in *Sphagnum* assemblage behaviour – for example, wetland sub-environments such as hummocks, hollows and pools have different assemblages of *Sphagnum* species

Geoscientific
Model Development
Discussions

although similarities also exist (Rydin 1986). However, DGVMs also require the number of PFTs to be limited, and previous studies (Druel et al. 2017; Qiu et al. 2018; Wania 2009a, 2009b; Yurova et al. 2007) have found improved fit of peatland ecosystem NPP with field CO_2 exchange data using very simple *Sphagnum* PFTs. Therefore, we sought to develop, as a first attempt, a single process-based *Sphagnum* PFT that has a higher level of detail than these previous studies in a current-

5 generation DGVM, having a consistent level of detail with existing vascular PFTs in the same DGVM. We chose the TRIFFID DGVM because it has very widespread use as part of JULES and the Hadley Centre Climate Model and it has been validated across many biomes (e.g. Clark & Gedney, 2008; Cox et al 1998; Cox et al 2001; Hughes et al 2004; Harper et al 2018). Despite its widespread use, however, a major advancement is needed in the functionality of the model by improving the representation of the peatland biome. This is because it does not have any module that reproduces the vegetation or hydrology

10 mechanisms of peatlands (e.g. see Harper et al's (2018) description of the vegetation types represented in a very recent version of JULES).

Other DGVMs that have simple *Sphagnum* PFTs incorporated are coupled to a peat-soil-model, and were validated as whole ecosystems not as individual PFTs. A *Sphagnum* plant respiration and production model was developed by Yurova et al (2007)

15 as a modification of the Lund-Potsdam-Jena General Ecosystem Simulator (LPJ-GUESS). The LPJ base-model is simpler than TRIFFID, lacking detail such as leaf-gas-conduction and therefore not making any model-code-level distinction between vascular and non-vascular plants. Therefore, LPJ's *Sphagnum* PFT just has different parameters without changing the base-code of the model. The ORCHIDEE-PEAT model (Qiu et al. 2018) uses its existing C3 grass PFT with stomatal gas-regulation to simulate peatland NPP, calibrating it at each site using locally measured V_{max} values (a key enzyme-controlled reaction rate

20 in photosynthesis dependent on the local environment as well as inherited properties of the plants). This local calibration against V_{max} is recognised by the authors as a major adjustment factor to cover multiple uncertain parameters, adjusting for the fact that non-vascular properties of some of the vegetation in the test-sites are not accommodated in the model code. Similarly, Druel et al (2018) in another version of ORCHIDEE used its existing C3 grass vascular model and parameters to simulate non-vascular plants (including all mosses as well as *Sphagnum* in a single PFT), modifying the parameters to minimise the effects

25 of stomatal regulation of leaf-gas exchange from the base vascular model, but short of changing the base model itself to resemble the non-vascular function of *Sphagnum*. These ORCHIDEE and LPJ sub-models represented whole peat-ecosystems including soil-processes and were validated against CO_2 -eddy-covariance measurements; they were not validated at the level of isolated individual PFTs. In this study, we have focussed on specific *Sphagnum*-processes instead of trying to approximate *Sphagnum*'s behaviour without changing the base model. This is to try to replicate *Sphagnum*'s production and respiration

30 mechanism in more detail than other DGVMs have done so far, at this isolated PFT level. For the first time with any non-vascular PFT as far as we are aware, this model should permit direct comparison with organism-level productivity and respiration measurements, permitting the first attempt at a general model for *Sphagnum* photosynthesis and respiration at this higher level of detail. Since this work does not include the development of a coupled peat-soil model then the model-output

cannot be validated against CO_2 eddy-covariance measurements (such as used by Qiu et al 2018) since we are not simulating whole-ecosystem NPP.

An increased level of functional detail is introduced in section 2 where we outline the key biological and physical traits of

5   *Sphagnum* that require new functions in TRIFFID, with an explanation of how we have incorporated specific *Sphagnum* traits within TRIFFID. We present the outputs of model runs in section 3. We test the model with available data from recently published studies, which measured assemblage-NPP, assemblage-GPP, assemblage respiration, WTP (water-table position), PAR (photosynthetically active radiation), temperature, canopy dark respiration and V_{max}. Canopy dark respiration is the respiration in leaves that occurs in cell mitochondria as opposed to photosynthesising cell components, and V_{max} is the

10   maximum rate of carboxylation of rubisco, which is a key photosynthesising enzyme that controls primary production. Section 4 concludes by outlining further potential developments of the new *Sphagnum* PFT model and its wider use.

2. Model development and theory

Sphagnum exchanges gas directly through cell walls. Individual *Sphagnum* stems and leaves are spongy and porous, and they grow in tightly packed assemblages. The surface shoots of these *Sphagnum* assemblages have been observed to retain a lot of

15   water in this way, having up to ten times as much water by mass as the dry-mass of the plants themselves (Hayward & Clymo 1982; Rydin 1985; Rydin & Jeglum 2006; Strack et al. 2009). This water is held and sucked up by capillarity in the surface *Sphagnum* matter and deeper *Sphagnum* litter (e.g. Charman 2002; Rydin & Jeglum 2006; Van Breemen 1995). These characteristics mean that *Sphagnum* plants have clear differences to vascular plants in terms of physical shape and the processes that occur within them. Where these characteristics are relevant to simulating photosynthesis and plant respiration (R_p) in a

20   PFT model, they are described in Table 1 in comparison to a pre-existing example of a vascular PFT that has been developed and tested in TRIFFID. Table 1, therefore, illustrates the basis for modifications that are required to incorporate *Sphagnum* within the TRIFFID DGVM.

Table 1. A comparison of *Sphagnum* processes with those of typical C3 vascular plants

Process	C3 Graminoids	*Sphagnum*
Life form	Able to survive as individuals across wide range of soil conditions, although few survive long periods total saturation. Consist of roots (below ground) and the shoot that has stems, leaves and seed-heads. Often exist in large assemblages with other grasses and other vascular plants.	Only ever occur in assemblages. Only exist where the soil normally has high moisture content and some species tolerate long periods of total saturation. Consist of closely packed branching stems. Along the stems are 'stem leaves' and the whole assemblage forms 'mats' where only the top few cm (the capitulum) receive enough light to photosynthesise.
Leaf anatomy	Several cell layers, water impermeable cuticula, punctuated with stomata.	Leaf is single cell layer containing photosynthesising and non-photosynthesising cells with no stomata.
Leaf-air gas exchange	Regulated by stomata that open fully or partially to specifically allow transpiration, but also conserve moisture by closing up under water-stress of the leaf or when there are strong humidity gradients.	Constant gas exchange via molecular diffusion between photosynthesising cells and either directly with atmosphere or via thin water-film between leaf and atmosphere.
Photosynthesis	C3 pathway	C3 pathway
Water uptake and transport	Xylem vessels connect the roots vertically to the leaves. Strongly negative water potential at leaf surface is due to transpiration from the leaf. Water drawn up under strong hydraulic gradients from roots. Waxy cuticula leaf surface prevents direct leaf-water uptake.	Water uptake and release from much of the plant surface. Vertical water transport occurs up the exterior of the stem, including deeper dead stem material, and underlying peat by capillary action. No clear dividing line between these formations. Assemblages also intercept and absorb water from direct precipitation.
Water storage and stress	Not desiccation tolerant. Metabolism might slow under stress but needs to be maintained. Water stored in living cells; high internal water storage is a requirement for plant structure and survival. Stomata close during drought to limit transpiration but high soil water tension leads to the plant being unable to access soil water, resulting in cell wall collapse and mortality.	Desiccation tolerant. Metabolism suspended until wet periods return. Quick to recover after drought. Water storage in spongy assemblages. The leaves consist of small living chlorophyllose cells and large structural dead hyaline cells that store lots of water. Closed canopy shelters underlying peat from direct sunlight. Peat typically has very high moisture content even after drought.

Geoscientific
Model Development
Discussions

2.1 Life form

Sphagnum assemblages exist at a spatial scale of up to $100 \, \text{km}^2$ (e.g. Baird et al. 2009; Bragg & Lindsay 2003; Rydin & Jeglum 2006). *Sphagnum* assemblages are closely packed 'mats' within which individuals, of the order of 10 cm in length, are vertically oriented. They are typically damp or saturated in their lower extents, and their leaves do not exhibit significant internal water transport and have no vascular system (Rydin et al. 2006, Rydin & Jeglum, 2006; Van Breemen 1995). Due to the lateral packing of the assemblages, only the top few centimetres of *Sphagnum* mats receive enough light to photosynthesise (Rydin & Jeglum, 2006). This photosynthesising surface section is called the capitulum. Different *Sphagnum* species show varying degrees of environmental tolerances and responses, and favour particular microenvironments of topography and wetness. Nevertheless, *Sphagnum* species show similar *forms* of reactions to variations in environmental drivers (Johnson et al. 2015).

2.2 Leaf anatomy and air-gas exchange

The one-cell-thick *Sphagnum* leaf has green photosynthesising cells that alternate with larger hyaline cells. The hyaline cells are rigid, transparent, porous, structurally support the plant, and store water through capillarity. The cells die when fully developed within the living plant, but they retain their structural and hydrological functions (Rydin et al. 2006, Rydin & Jeglum 2006). There is no active control of the rate of the conductance of any substance between the photosynthesising cells in *Sphagnum* and the atmosphere (Rydin & Jeglum 2006). These photosynthesising cells are directly in contact with the atmosphere or submerged under water. This is different to vascular plants, which have an opening and closing apertures in the leaf surface that permit atmospheric exchange (e.g. Amthor & Baldocchi, 2001).

2.3 Photosynthesis

There are several different sets of processes within the photosynthesising cells of different types of plants, but each plant type exhibits only one such carbon fixation pathway. The most common is the C3 carbon fixation pathway, which *Sphagnum* also shows (Loisel, et al. 2009; Price, et al. 1997). R_p is equal to the carbon lost to the atmosphere because of energy use by the plant including respiration from leaves, stems and roots. GPP is equal to the carbon that is fixed by photosynthesis as carbohydrate. NPP is the arithmetic difference between GPP and R_p, which results in the physical growth of the plant through the net assimilation of carbon (Amthor & Baldocchi, 2001; Begon, et al. 2005).

2.4 Water transport, storage and stress

Sphagnum plants store water within densely packed stems and leaves, incorporating hyaline cells. The volume stored varies between species (Rydin & Jeglum 2006). Capillarity enables vertical water transport to occur up the exterior of the stem from the underlying peat, including along deeper dead *Sphagnum* material (Hayward and Clymo 1982; Rydin & Jeglum 2006; Van

5   Breemen 1995). There is very little internal vertical water transport within the stems. The assemblages also intercept and absorb water from direct precipitation (Hayward and Clymo 1982; Rydin & Jeglum 2006; Thompson & Waddington 2008; Van Breemen 1995), while the closed canopy shelters underlying peat from direct sunlight (Bu et al. 2013; Charman 2002). *Sphagnum* is desiccation-tolerant, and it suspends its metabolism until wet periods return after which it is quick to recover after drought (Hájek & Beckett 2008).

10

2.5 Model components

Given the above information, we take as a template the carbon exchange equations of TRIFFID and modify them according to specific characteristics of *Sphagnum*. There are six processes and mathematical process descriptions, in Tables 1 & 2. The new model does not explicitly accommodate water storage, transpiration, desiccation-tolerance or variable *Sphagnum* canopy

15   CO_2 uptake and release related to microform position (Wania et al. 2009b). These would require new process understanding and datasets and so they have not been addressed in this version of the TRIFFID *Sphagnum* PFT model. However, there are 11 important changes to the parameters of the model. Seven parameters were developed using published field and laboratory studies (Table 3), and four used as shaping parameters (Table 4). The following paragraphs describe this parameter development.

20

The new PFT model simulates photosynthesis of a *Sphagnum* assemblage, which is not simply scaled up individual-behaviour. This is shown in a new empirical water-uptake equation (the right-hand-column for point 1 in Table 2) which simulates the assemblage-water-uptake mechanism (as described in section 2.4). It is based on a similar mechanism for vertically distributed vascular roots in existing TRIFFID vascular PFTs (Cox et al 1998). Cox et al. (1998) found that this has the advantage of

25   programmatic simplicity, employing fewer variables than explicit simulation of water-uptake, whilst still giving a good model fit. This approach directly utilises the unitless volumetric water content of the photosynthesising *Sphagnum* capitulum as the desiccation-stress factor. The specific desiccation stress factor for the new *Sphagnum* PFT model was based on field observations derived from Strack et al. (2009) who plotted an empirical function of capitulum water content against the water-table position (WTP) for *Sphagnum* assemblages and who also found a strong linear relationship between surface volumetric

30   moisture content and assemblage production. Murray et al. (1989) and Riutta et al. (2007), studying bog ecosystems in the foothills of the Philip Smith Mountains, Alaska, and the Lakkasuo bog in southern Finland, respectively, recognised that the maximum *Sphagnum* photosynthetic production value occurs when the water table is just below the ground surface. A fixed

maximum value was therefore used to reproduce this, when the WTP is less than 10 cm below the ground surface, incorporated as a limit in the *Sphagnum* equation shown on the right-hand-column for point 1 in Table 2. This new *Sphagnum* equation provides an overall non-vascular desiccation-stress function, which replaces Cox et al's (1998) vascular desiccation-stress function on the left column of point 1 in Table 2. For leaf air-gas exchange, where a simple scaled-up 'big leaf' approach is

5 used, a fixed value for leaf conductance has been applied in the new *Sphagnum* PFT model, replacing the variable stomatal conductance used in the TRIFFID vascular PFT model (point 2 in Table 2). This approach is in place of Williams & Flanagan's (1998) explicit simulation of varying *Sphagnum* leaf conductance, abstracting away from their higher level of detail in favour of reduced model-complexity (for example dead *Sphagnum* matter capillarity at the top of the soil column is not incorporated in any DGVMs yet). This follows similar successful approaches in Cox et al. (1998) for vascular plants, and Wania et al.

10 (2009b) and Yurova et al (2007) for *Sphagnum* growth in the LPJ model.

The equations that simulate photosynthesis and respiration processes that occur within cells, which are unchanged by assemblage-behaviour, are in points 3 and 4 in Table 2. To simulate the photosynthesis biochemical pathway in the new *Sphagnum* model, the existing C3 carbon fixation function within the TRIFFID vascular PFT sub-model was used to form the

15 basic model. GPP for vascular PFTs is simulated in TRIFFID, as in many other DGVMs, as a function of the minimum of three limiting rates to fix carbon within the photosynthesising cells of a leaf (Clark et al. 2011). These are the light limited rate GPP_l, the Rubisco-limited rate, GPP_r, and the rate of transport of photosynthetic products by the plant, GPP_e, which are simulated using the equations on the left-hand column for point 3 in Table 2. In the new *Sphagnum* model, the conductance between the atmosphere and *Sphagnum's* photosynthesising tissues is a fixed value representing permanent exposure of the

20 tissues to the atmosphere, resulting in a similar approach to Druel et al. (2017) and Dimitrov et al. (2011) to simulating non-vascular plants' leaf-conductance. The solutions for internal leaf partial pressure (c_{ri} and c_{li} respectively) as functions of the photosynthesising processes in the leaf and atmospheric pressure are then solutions of the quadratic equation given on the right-hand column for point 3 in Table 2, thus giving solutions for GPP_r and GPP_l by substitution. A smoothed minimum value to simulate overall GPP (using the existing TRIFFID smoothing function in simple form on the left-hand column in point 3 of

25 Table 2, and in detailed form in Appendix A) is then calculated from these two values (and the unaltered photosynthetic product transport-limited GPPe). The plant respiration equations (point 4 in Table 2) are unchanged, but the parameters saw significant changes, see sub-section 2.6.

The gas assimilation-inflow continuity equation and surface energy balance equation (respectively points 5 and 6 in Table 2)

30 are unchanged as these describe simple physics that should be the same between non-vascular *Sphagnum* and vascular plants.

The new *Sphagnum* PFT model requires changed parameters because *Sphagnum* has different physical dimensions to the other PFTs already represented in TRIFFID. As a result, there were 11 changes to PFT parameters needed in the new TRIFFID *Sphagnum* PFT model (Tables 3 and 4). Of the physiology parameters (Table 3), three are parameters for *Sphagnum* respiration

taken from observation-based parameters tested in LPJ-GUESS (N10, T_{upp}, T_{low}) while four have had their values established from existing field and laboratory literature on *Sphagnum* (tleaf_of, infil_f, catch0, Canht_ft). We could not find precise data to constrain the parameters LAI, fd and rg (Table 4) so they were used to shape the output respiration function to the output field data. For example, Yurova et al. (2007) and Bond-Lamberty & Gower (2007) give rough ranges for these parameters.

5   Appendix B provides the detailed steps taken to set the shaping parameters, which resulted in an initial calibrated model whose outputs are in section 3.

Geoscientific
Model Development
Discussions

Table 2. Processes and mathematical descriptions of carbon exchange plant growth in C3 PFTs in TRIFFID and the modifications made to them according to the specifics of *Sphagnum* for the new *Sphagnum* PFT model.

TRIFFID – C3 vascular plant

(1) Carbon gain of plant – mass balance

$$A = (GPP - R_d)\beta$$

$$\beta_{vascular} = \sum \begin{Bmatrix} 1, & \theta > \theta_c \\ \dfrac{\theta - \theta_w}{\theta_c - \theta_w}, & \theta_w < \theta \leq \theta_c \\ 0, & \theta > \theta_w \end{Bmatrix}$$

$\beta_{vascular}$ is summed for all the soil layers underlying the PFT

(2) Stomatal conductance

$$g_s = \frac{\alpha A}{(c_{atm} - \Gamma)\left(1 + \dfrac{D}{D_0}\right)}$$

'Simplified Leuning model' - the Leuning (1995) model of stomatal conductance in a vascular plant, was simplified by Cox et al. (1998) by setting optimal minimum canopy conductance to zero.

(3) Photosynthesis machine

$$GPP \approx min(GPP_r, GPP_l, GPP_e)$$

$$GPP_r = V_m\left(\frac{c_i - \Gamma}{c_i + K_c(1 + O_a/K_0)}\right)$$

$$GPP_l = 0.08(1 - \omega)I_{par}\left(\frac{c_i - \Gamma}{c_i + 2\Gamma}\right)$$

$$GPP_e = 0.5V_m$$

$$\Gamma = \frac{O_a}{2\tau}$$

$$\tau = 2600f_T(0.57)$$

Sphagnum (see Appendix A for derivations)

Has the following changes:

$$\beta_{Sphagnum} = \begin{cases} 1, & WTP > -0.1m \\ e^{\left(\frac{0.1 + WTP}{0.16}\right)}, & WTP \leq -0.1m \end{cases}$$

Has the following changes:

$$g_s = 1.6 * 0.0237 * 0.07 \, ms^{-1}$$

Has the following changes:

$$GPP_r = V_m\left(\frac{c_{ri} - \Gamma}{c_{ri} + K_c(1 + O_a/K_0)}\right)$$

$$GPP_l = 0.08(1 - \omega)I_{par}\left(\frac{c_{li} - \Gamma}{c_{li} + 2\Gamma}\right)$$

$$c_{ri}, c_{li} = \frac{-BB + \sqrt{BB^2 - 4AACC}}{2AA}$$

$$AA_r = \frac{G}{V_m} \ , \ AA_l = \frac{G}{I} \quad BB_r = \frac{G}{V_m}(K - c_{atm}) - R_d + 1$$

$$f_T(T_c) = q_{10\_leaf}^{0.1(T_c-25)}$$

$$BB_l = \frac{G}{I}(2\Gamma - c_{atm}) - R_d + 1$$

$$CC_r = -\left(\frac{G}{V_m}Kc_{atm} + KR_d + \Gamma\right)$$

$$CC_l = -\left(\frac{G}{I}2\Gamma c_{atm} + 2\Gamma R_d + \Gamma\right)$$

where the following simplifying terms are used:

$$G = \frac{g_s}{1.6\bar{R}T^*\beta}, \quad I = 0.08(1-\omega)I_{par}, \quad K = K_c\left(1 + \frac{0_a}{K_0}\right)$$

(4) Respiration

$$R_p = r_g(\Pi_G - R_{pm}) + R_{pm}$$

(plant respiration = growth respiration + maintenance respiration)

Equations unchanged, new parameters taken from tested *Sphagnum* parameters in LPJ-GUESS/WHY which in turn were originally based on field data (see appendix B).

$$R_{pm} = 0.012 \cdot R_{dc}\left(\beta + \frac{N_r + N_s}{N_l}\right)$$

(maintenance respiration)

$$R_d = f_d \cdot V_m$$
$$R_{dc} = \sum(R_d)$$

(canopy dark respiration)

(5) Continuity equation

Assimilation = inflow

$$A = \frac{g_s}{1.6\bar{R}T_*}(c_{atm} - c_i)$$

Unchanged

(6) Surface energy balance

$$R_S = SW_N + LW_\downarrow - \sigma T*^4 - H - LE - G_0$$

Unchanged

Parameter names in this table:

A - net leaf photosynthesis (mol CO_2 m^{-2}s^{-1})

11

AA, BB, CC – quadratic equation parameters

AA_r, BB_r, CC_r - quadratic equation parameters for case of Rubisco-limitation of GPP

AA_l, BB_l, CC_l - quadratic equation parameters for case of light-limitation of GPP

c_{atm} - atmospheric CO_2 partial pressure (Pa)

c_i - internal leaf CO_2 partial pressure (Pa)

c_{ri} – Rubisco-limited internal leaf CO_2 partial pressure (Pa)

c_{li} – light-limited internal leaf CO_2 partial pressure (Pa)

D - Humidity deficit at the leaf surface (g kg^{-1})

D_0 - Leaf surface humidity deficit parameter for the 'Leuning' closure (g kg^{-1})

f_d - the dark respiration scaling factor

fT - the standard Q10 temperature dependence

g_s – leaf surface conductance (stomatal conductance in vascular plants) (ms^{-1})

G, I, K – terms to simplify the layout of equations in the *Sphagnum* photosynthesis machine

GPP – leaf Gross Primary Production (mol CO_2 $m^{-2}s^{-1}$)

GPP_e – GPP rate limited by transport of photosynthetic products by the plant (mol CO_2 $m^{-2}s^{-1}$)

GPP_l – light limited rate of GPP (mol CO_2 $m^{-2}s^{-1}$)

GPP_r – Rubisco-limited rate of GPP (mol CO_2 $m^{-2}s^{-1}$)

G_0 – heat flux into the ground (see Best et al. (2011) for detail inside this term) (Wm^{-2})

H – sensible heat flux (Wm^{-2})

I_{par} - incident photosynthetically active radiation (mol photons m^{-2} s^{-1})

K_c, K_0 - Michaelis Menten parameters for CO_2 and O_2 (Pa) (see Clark et al. (2011))

LE – heat flux due to evapotranspiration (latent heat of vaporisation, L x moisture flux, E) (Wm^{-2})

$LW_↓$ - incoming longwave radiation (Wm^{-2})

N_l - nitrogen content of leaf portion of plant (mol CO_2 m^{-2} s^{-1})

N_r - nitrogen content of root portion of plant (mol CO_2 m^{-2} s^{-1})

N_s - nitrogen content of stem portion of plant (mol CO_2 m^{-2} s^{-1})

O_a - partial pressure of atmospheric oxygen (Pa)

Q10_leaf – Q10 temperature dependence coefficient

r_g – growth respiration coefficient

R_{pm} - plant maintenance respiration (kgC $m^{-2}s^{-1}$)

R_d - leaf dark respiration (mol C $m^{-2}s^{-1}$)

R_p – plant respiration (kg C $m^{-2}s^{-1}$)

R_S – surface energy balance (Wm^{-2})

R_{dc} - canopy dark respiration (mol C $m^{-2}s^{-1}$)

SW_N – balance of shortwave radiation (Wm^{-2})

$T_{c\,-}$ canopy (leaf) temperature (°C)

T_* - the leaf surface temperature (K)

V_m – temperature-dependant maximum rate of carboxylation of the Rubisco enzyme (CO_2 m^{-2} s^{-1})

WTP – water table position (m)

α - Quantum efficiency [mol CO_2 (mol PAR, photons)$^{-1}$]

β - desiccation stress factor, unitless ($0 \leq \beta \leq 1$)

Π_G – PFT-canopy GPP rate (kgC $m^{-2}s^{-1}$)

θ - mean soil water concentration in the root zone

θ_c, θ_w - vascular PFT-specific critical and wilting soil moisture concentrations respectively

σ - Stefan Boltzmann constant (Wm^{-2} K^{-4})

τ - Rubisco specificity for CO_2 relative to O_2

Γ - CO_2 photorespiration compensation point (Pa)

ω - the leaf scattering coefficient for PAR

Table 3. TRIFFID PFT constrained physiology parameters changed for the new *Sphagnum* PFT model.

Function	Symbol	Value	Description / references
Canopy Height	Canht_ft	0.03m	Height of leaves above ground (Smolders, et al. 2001)
Minimum canopy capacity	catch0	0.25 kg m^{-2}	Bond-Lamberty & Gower (2007)
Infiltration enhancement factor.	infil_f	1.0	Reduced compared to grasses (2.0) reflecting lower hydraulic conductivity
Top leaf nitrogen concentration	Nl0	0.02 kg N/kg C	Wania, et al. (2009b) (Wania, 2007), in approximate agreement with (Rice 2000) and Aerts et al (2009)
Temperature below which leaves are dropped	tleaf_of	0 Kelvin	Representing no lower limit
Lower temperature for photosynthesis	Tlow	5.0 Celsius	Gerdol, et al. (1998); Wania, et al. (2009b)
Upper temperature for photosynthesis	Tupp	36.0 Celsius	Gerdol, et al. (1998); Wania, et al. (2009b)

Geoscientific
Model Development
Discussions

Table 4. TRIFFID PFT physiology shaping parameters for the new *Sphagnum* PFT model, compared with equivalent parameters in LPJ-GUESS *Sphagnum* PFT.

Function	Symbol	Value	
		LPJ-GUESS	TRIFFID
Dark Respiration Scaling Factor	f_d	0.03	0.03
Growth Respiration Coefficient	r_g	0.5	0.1
Non-Photosynthetic Tissue Respiration	r_m	2.0	Not used
Leaf Area Index	LAI	Not used	3, hummock/bog species
			1, lawn/fen species

2.6 Model Calibration

Table 5. Literature sources of quantified *Sphagnum* respiration and photosynthesis functions.

Reference	Model Functions Adopted in the new *Sphagnum* PFT model *[Functions used for output comparisons]*	*Sphagnum* species quantified	Season when measurements taken
Aerts et al (2009)	Leaf nitrogen concentration	*S Fuscum*	Summer
Hayward & Clymo (1982)	Capitulum volumetric water content against WTP, similar shaped function to Strack et al. (2009) (below)	*S. Capillifolium* *S. Papillosum*	Not given
Murray et al. (1989)	Photosynthetic maximum at near surface water table, agrees with Riutta et al.(2007) (below)	*synthesised studies of many arctic species*	Summer
Rice (2000)	Leaf nitrogen concentration	*S. Recervum* *S. Palustre* *S. Tenerum*	Spring and summer
Riutta et al. (2007)	Photosynthetic maximum at near surface water table, but photosynthetic and respiration responses are otherwise approximately flat against WTP *[NPP against WTP, temperature and PAR]*	*S. Papillosum* *S. Fallax* *S. Flexuosum*	'Growing season'
Strack et al. (2009)	Capitulum volumetric water content against water table position, after first order correction for presence of vascular vegetation *[NPP against WTP]*	*S. Rubellum*	Very late spring, summer
Williams & Flanagan (1998)	Maximum leaf CO_2 conductance *[Cell dark respiration and Vm]*	*S. Rubellum* *S. Tenellum* *S. Capillifolium* *S. Fuscum*	Summer

5

We could only find one set of data that was useful for general model calibration (Table 5 – Strack et al. 2009) and two for validation (Table 5 – Riutta et al. 2007; Williams & Flanagan 1998). The remaining data sets listed in Table 5 either gave very similar data to these three sources, or individual parameters for the model. Strack et al (2009) presented GPP and R_p field-data

5   from a *Sphagnum*-dominated bog ecosystem (nutrient-poor peatland with a shallow to deep water-table) in late spring and summer. Having GPP and R_p disaggregated was very useful for calibrating our detailed *Sphagnum* model, and as far as we are aware, these data are the only such published data. Strack et al (2009) studied a mixed ecosystem with at least 90% *Sphagnum* cover, so, unfortunately, the field-data did not represent isolated *Sphagnum* behaviour. However, we found a first-order correction, based on data from Riutta et al (2007), who showed that peatland vascular vegetation NPP (which is GPP-R_p)

10 against WTP is approximately horizontal, or uncorrelated. Additionally, Riutta's *Sphagnum* GPP data asymptotically approaches zero for deep water tables, which leads to desiccation of the capitulum, a theory supported by observations from Bewley et al. (1978), Hájek & Beckett (2008) and Hayward & Clymo (1982). Therefore, a first order correction was applied by simply subtracting a fixed positive offset (assumed to represent the influence of vascular plants) from the R_p and GPP data of Strack et al (2009) so it has R_p and GPP approaching zero for very low WTP values. The resultant NPP data was in this way

15 transformed to give the calibration data shown in Figure 1.

Our model was calibrated to reproduce the transformed GPP, NPP and R_p data of Strack et al (2009). We used fixed environmental model-inputs (PAR, temperature and WTP), running the model like a controlled laboratory without varying climate inputs. r_g (growth respiration coefficient – see Table 4) was adjusted to set the R_p curve in the correct position. The

20 NPP curve merely is the algebraic sum of these two curves. This parameter-fitting exercise is described fully in Appendix B. The outcomes are in Figure 1.
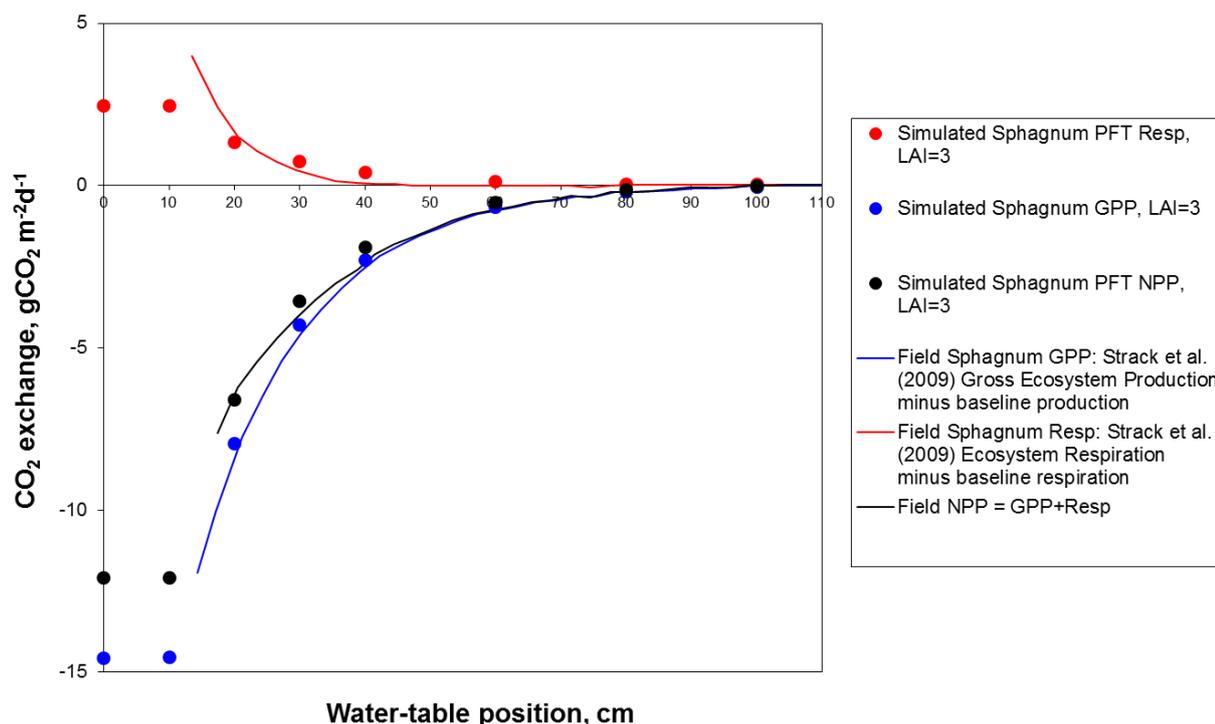
Figure 1. Model outputs of respiration, GPP, and NPP against WTP, calibrated with field measurements from a *Sphagnum*-dominated peatland constructed using data derived from Strack et al (2009).

3. Results

5   The calibrated *Sphagnum* PFT model was tested against the limited data available from Riutta et al (2007) and Williams & Flanagan (1998) and gave good visual matches against these quite complex measured functions of varying ecosystem productivity and respiration. The degree of fit was not measured quantitatively, because getting the shape of all the various output functions of the model right was a much higher priority than the accuracy of fit, and the test-data is very limited. The model reproduced the shape of the seven different curves in both calibration

10   and test datasets with a limited amount of fine tuning.

Riutta et al (2007) measured GPP of mixed peatland vegetation in a nutrient-poor fen (peatland with a shallow water-table fed by lateral inflows). They isolated *Sphagnum* GPP but not R_p or NPP, at a field plot during the

growing season. This was not a time series such as is common in ecosystem CO_2 eddy-covariance measurements, but rather as isolated functions of GPP against PAR, temperature and WTP. Our model was, therefore, run using fixed environmental model-inputs (PAR, temperature and WTP) to reproduce *Sphagnum* GPP functions against temperature and PAR, to simulate the Riutta data. One change was required to the LAI parameter to accommodate

5   the different *Sphagnum* species to the earlier calibration data, explained in Appendix B.2. We note that this curve-fitting factor may have corrected more than just the LAI differences between *Sphagnum*-species, which is further addressed in section 4. The model output is therefore compared to the Riutta test-data in figure 2.

Also, non-desiccation-stressed full daylight canopy dark respiration within the TRIFFID *Sphagnum* model was

10   between 0.4 µmol m^{-2}s^{-1} (LAI=1, fen *Sphagnum*) and 0.7 µmol m^{-2}s^{-1} (LAI=3, bog *Sphagnum*). V_{max} is a fixed value in the model of 16 µmol m^{-2}s^{-1} from equation A.11, being proportional to the leaf nitrogen content value, nl (kgNm^{-2}), which is a fixed value in the model. These values compare well with Williams & Flanagan's (1998) average daylight summer laboratory measurements of a truncated bog/poor fen *Sphagnum* sample with an uncertain LAI, giving a value for canopy dark respiration of 1.0±0.3 µmol m^{-2}s^{-1} (at one standard deviation) and a value for V_{max}

15   of 14.0±4.0 µmol m^{-2}s^{-1}.

Thus, using available field or laboratory data, our *Sphagnum* PTF model visually reproduces the shape of laboratory-derived *Sphagnum*-CO_2 exchange curves, but with some clear residuals of up to about 40% against WTP and temperature, and up to +100% against PAR. The significant amount of detailed work performing the above

20   calibrations and testing is described in Appendices 1 & 2.
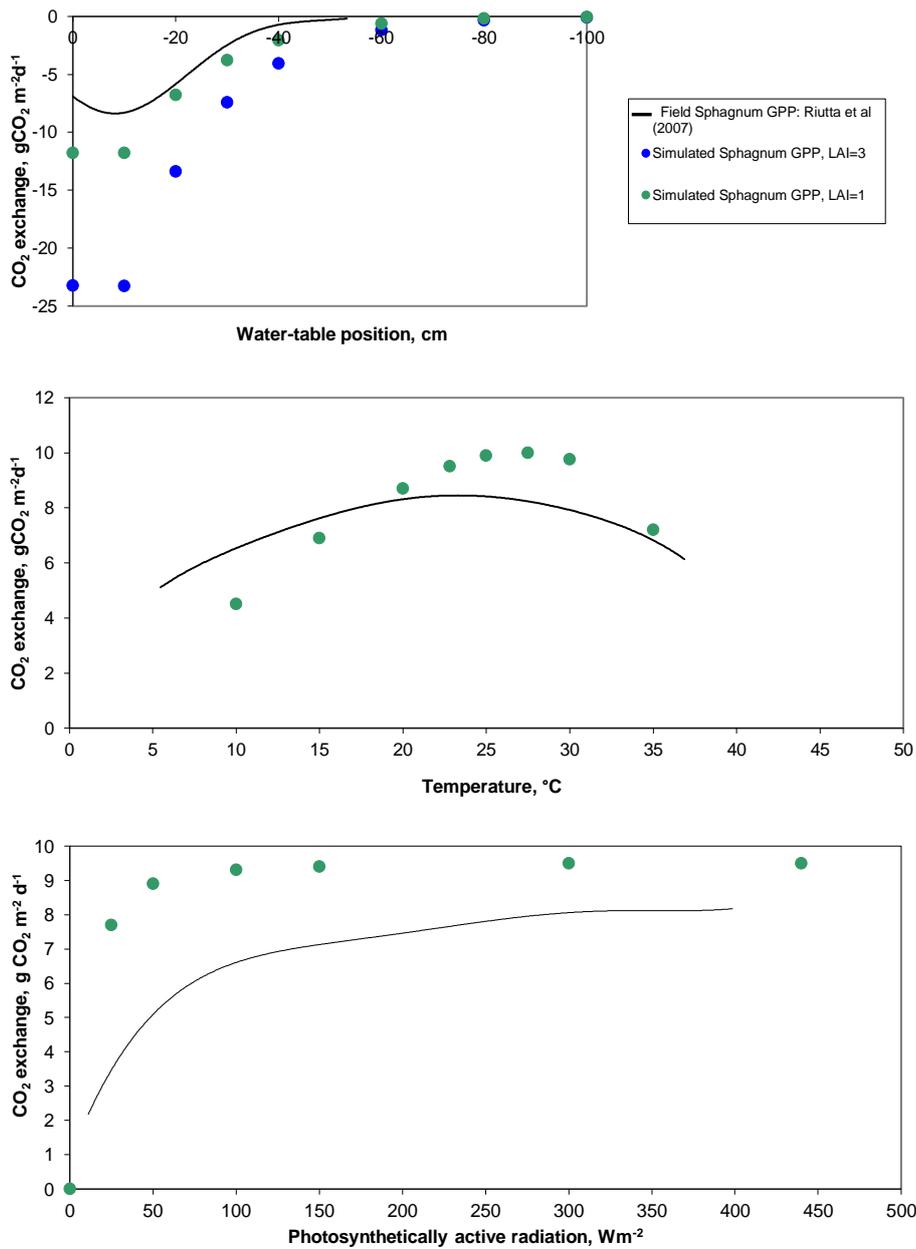
Figure 2. Model outputs of GPP against WTP, temperature, and PAR, compared to field data from a *Sphagnum*-dominated peatland obtained by Riutta et al (2007).

Geoscientific
Model Development
Discussions

4. Discussion and Conclusions

A new process-based non-vascular-PFT model has been developed. *Sphagnum* mosses exhibit characteristic curves of R_p, GPP and NPP against WTP, PAR and temperature that are very markedly different to vascular plants (see

5   Riutta et al. 2007). The new *Sphagnum* model reproduced the overall shape of these *Sphagnum* curves without any calibration. We believe this is the first time any process-based non-vascular plant photosynthesis model has reproduced these distinct curves. The model required only r_g adjusting in order to calibrate it to the data from Strack et al (2009). Only a simple adjustment of the LAI parameter, being well supported by the literature to accommodate a different *Sphagnum* species, allowed our model to reproduce Riutta et al's (2007) GPP curves against WTP and

10   temperature within about ±40% of the field-measurements. The fit to Riutta's PAR curve was less accurate at between +20% and +100% residual. We did not attempt any closer fitting here because this was intended to be test data to validate the initial calibration against the Strack data. There is insufficient test data to support statistical analysis of the residuals, with only a small number of features in the test-data curves. However, we also note that no previously published process-based models that we could find of *Sphagnum* photosynthesis (Druel et al. (2017),

15   Qiu et al. (2018), Wania et al. (2009a, 2009b) and Yurova et al. (2007)) made any comparison to isolated field *Sphagnum*-NPP data, so our model is a first attempt at a greater level of process-detail together with a direct comparison to this field data. Of course, more field data would be welcome to improve confidence and to help refine the model.

Furthermore the use of LAI and r_g as curve-fitting factors may accommodate a broad range of uncertainty elsewhere

20   in the fitting of the model parameters, including, for example, varying photosynthetic efficiency of different *Sphagnum* species, internal near-surface water storage, transpiration, and varying CO_2 transport pathways available through pore-water and the atmosphere to the *Sphagnum* capitulum (Proctor et al, 1992; Lamers, 1999; Limpens et al 2008). These are little understood and therefore not candidate functions to be included in the *Sphagnum* PFT model in the foreseeable future.

25

Improved *Sphagnum* NPP models offer the possibility of simulating the accumulation of peatland plant litter with varying decomposition recalcitrance values and hydraulic properties (Wania, et al. 2009a), which influence the stability of the peat soil carbon store (Belyea 2009; Frolking et al. 2001). These two points are consistent with the observation of complex feedbacks between plant physiology and soil moisture (Bevan 2012) and Laurent et al.'s

(2004) view that, in order to improve the accuracy of existing vegetation carbon cycling simulations, simple climate-correlation (Brovkin et al. 1997; Prentice et al. 1992) may be enhanced by the inclusion of non-climate factors including plant-soil feedbacks. Additional parameters to be integrated within the model could be, for example, nutrient content (the nitrogen cycling is already represented in some other bryophyte models, e.g.

5 Euskirchen et al. 2009), intra-annual flood-frequency as already simulated explicitly in LPJ-WHY (Wania, et al. 2009b) and implicitly in JULES (O'Connor et al. 2010), and the influence of small-scale land topography on vegetation assemblage functions at higher scales (Baird et al. 2009; Belyea & Baird 2006; Sonnentag et al. 2008; Waddington & Roulet 1996).

10 Additionally, field and laboratory measurements show that *Sphagnum* V_{max} has significant seasonal variation. All of the literature sources used to calibrate the photosynthetic and respiratory function of our model collected their data from *Sphagnum* samples taken during summer (see Table 5). Hence, the seasonal pattern of *Sphagnum* photosynthesis cannot be produced by this initial version of the TRIFFID *Sphagnum* model. Williams & Flanagan (1998) measured reduced V_{max} values in spring and autumn, at half the summer value. This can be ascribed to a

15 summer maximum concentration of photosynthesising tissue (Skre & Oechel, 1981). Leaf nitrogen content is strongly correlated with plant photosynthesising capacity (Woodward 1994). Rice (2000) measured seasonal changes in the capitulum carbon to nitrogen ratio in three *Sphagnum* species that occupy contrasting niches on a temperate wetland in North Carolina. This showed a clear trend of increasing capitulum nitrogen concentration compared to carbon, which is strongly indicative of nl, leaf nitrogen concentration, between March and September,

20 and suggests that nl in *Sphagnum* should follow a seasonal pattern with a maximum value in summer. Therefore, the introduction of seasonally varying nl in place of the current fixed value in the model, is a candidate for future simulation of seasonal changes to *Sphagnum* V_{max}. Furthermore, while the quantum efficiency value in this model has been maintained at the C3 value of 0.08, used in JULES vascular PFTs, Kangas et al (2014) have measured quantum efficiency values for *Sphagnum* between 0.09 and 0.12 seasonally (with a minimum in July) and across

25 different *Sphagnum* species, but not correlated with local environment variables.

While the main focus of this paper has been the development of the new TRIFFID *Sphagnum* PFT model, the model we have produced is also readily suited to simulate true mosses, which play an important role in boreal ecosystems overlying unsaturated soils (Bond-Lamberty et al. 2004; Wieder, et al. 2006, Beringer et al 2001; Lindo

& Gonzalez 2010; Street et al. 2013). However, true mosses generally hydrate due to capillarity in their lower portions, distillation from a nocturnal temperature inversion of the underlying soil surface in their upper portions, or direct interception of precipitation (Carleton & Dunham, 2003; Lindo & Gonzalez 2010). This would require the replacement of the empirical water-uptake equation (point 1 in table 2) with a function reflecting this different

5   moisture-uptake mechanism, which is a relatively minor modification to the new *Sphagnum* non-vascular PFT. Precise quantification of this function does not yet appear to have been made empirically or theoretically, and this would be an important next step in enabling the adaptation of the current model to true mosses.

The most important outcome of this study is to have, for the first time, computationally solved the two-way

10   simultaneous function that governs photosynthesis in the non-vascular *Sphagnum* plant, thus simulating photosynthetic and respiratory functions of *Sphagnum*, which differ significantly from equivalent vascular vegetation functions, reproducing visually the NPP functions of *Sphagnum* samples. In other words we have developed, for the first time, a *Sphagnum* NPP model that resembles the internal function of the actual *Sphagnum* NPP mechanism, at a higher level of detail than existing PFT models such as those produced by Druel et al.

15   (2017), Qiu et al. (2018), Wania et al. (2009a, 2009b) and Yurova et al. (2007). Our work may therefore also contribute to a general photosynthesis model for *Sphagnum* beyond the immediate needs of DGVMs. It has been implemented in an existing latest-generation DGVM at a consistent level of detail and computational efficiency with the DGVM, but not coupled with the land-surface-functions of the DVGM such as hydrology and soil development, so it has not been possible to compare outputs to ecosystem eddy-covariance time-series.

20   Nevertheless even as it stands, the new model can be a tool to examine the carbon cycling patterns of *Sphagnum* under different climates.

Appendix A. Simulation of net leaf photosynthesis

A.1   Adaption of TRIFFID's C3 Photosynthesis Function to *Sphagnum*

Sphagnum exhibits the C3 carbon fixation photosynthesis pathway (Loisel, et al. 2009; Price, et al. 1997; Proctor et al. 1992). The TRIFFID vascular PFT with C3 carbon fixation has been adapted to replicate the non-vascular
5   *Sphagnum* photosynthesis function. This involved replacing the stomatal regulation of gas exchange in the model with a fixed leaf conductance value, and removing the ability to extract water from deep in the soil using a vascular root system.

The TRIFFID functions that were adapted to newly simulate *Sphagnum* physiology are summarised here from Best
10 et al. (2011) and Clark et al. (2011) (equation numbers with asterix). In TRIFFID, net leaf photosynthesis A (mol CO_2 $m^{-2}s^{-1}$) is computed using the solution to equations A.1 to A.6. GPP is the gross leaf photosynthesis, β is the desiccation stress factor, a unit-less value between 0 and 1, simulated for vascular plants using equation A.6, where Θ is the mean soil water concentration in the root zone, and Θ_c, Θ_w are the PFT-specific critical and wilting soil moisture concentrations respectively. Cox et al. (1998) showed that the simple desiccation-stress function in
15 equation A.1 improved the fit of a vascular vegetation model for a minimal number of extra parameters. R_d is dark respiration (see section 1), which is a linear function of V_{max} and f_T. c_{atm} is the atmospheric CO_2 partial pressure (Pa), and c_i are the rubisco- and light-limited potential internal leaf CO_2 partial pressures. O_a is the atmospheric oxygen (O_2) partial pressure (Pa). R is the ideal gas constant, T* is the leaf surface temperature (K), Γ is the CO_2 photorespiration compensation point (Pa) where photosynthesis balances respiration. In TRIFFID this is simulated
20 as a function of O_a and the Rubisco specificity of CO_2 relative to O_2, f_T f_T , equations A.7 and A.8. ω ω is the leaf scattering coefficient for PAR, for which TRIFFID assumes ω ω = 0.15 for C3 plants, and the value 0.08 in equation A.4 represents the quantum efficiency of C3 plants, α. Equation A.2 is the CO_2 diffusion equation.

For vascular plants exhibiting C3 photosynthesis, TRIFFID solves equations A.2 to A.5 as three simultaneous
25 functions of leaf surface gas conductance (equation A.2), gross photosynthetic rate, GPP, and stomatal closure, which is a function of the leaf humidity deficit – see Table 2 (Cox et al 1998). GPP is calculated using a smoothed minimum of GPP_r , GPP_l , and GPP_e (equation 1), which are GPP under photosynthetic-enzyme (Rubisco) limitation, light limitation, and photosynthetic-electron-transport limitation respectively, equations A.3 to A.5,

where Clark et al. (2011) in TRIFFID follows Sellers et al. (1996) and Cox et al. (1999). The three unknowns that are resolved, by the existing TRIFFID vascular PFT function, are A, c_i, and g_s.

$$A = (GPP - R_d)\beta \tag{A.1*}$$

$$A = \frac{g_s}{1.6RT_*}(c_{atm} - c_i) \tag{A.2*}$$

$$GPP_r = V_m\left\{\frac{c_i - \Gamma}{c_i + K_c(1 + 0_a/K_0)}\right\} \tag{A.3*}$$

$$GPP_l = 0.08(1 - \omega)I_{par}\left\{\frac{c_i - \Gamma}{c_i + 2\Gamma}\right\} \tag{A.4*}$$

$$GPP_e = 0.5V_m \tag{A.5*}$$

$$\beta_{vascular} = \begin{cases} 1, & \theta > \theta_c \\ \frac{\theta - \theta_w}{\theta_c - \theta_w}, & \theta_w < \theta \le \theta_c \\ 0, & \theta > \theta_w \end{cases} \tag{A.6*}$$

$$\Gamma = \frac{O_a}{2\tau} \tag{A.7*}$$

$$\tau = 2600f_T(0.57) \tag{A.8*}$$

$$f_T(q_{10}) = q_{10}^{0.1(T_c - 25)} \tag{A.9*}$$

V_m is calculated in equation A.10, and is a function of the lower and upper PFT–temperature production limits, T_{upp} and T_{low} and Q10 temperature dependence, f_T, the non-temperature-dependent rate, V_{max}, that simulates nitrogen-limitation of C3 photosynthesis (Clark et al. 2011) and leaf surface temperature, T_c. V_{max}, equation A.11 is kept the same for *Sphagnum* and other C3 plants following the example of Yurova, et al. (2007), and is a linear function of leaf nitrogen concentration, nl (kgNm-2).

$$v_m = \frac{v_{max}\ f_T(2.0)}{\left(1 + e^{0.3(T_c - T_{upp})}\right)\left(1 + e^{0.3(T_{low} - T_c)}\right)} \tag{A.10*}$$

$$v_{max} = 0.0008nl \quad \text{for C3 plants including } Sphagnum \tag{A.11*}$$

A.2 Gas Exchange Formulation for *Sphagnum* PFT

g_s *Sphagnum* applied to equation A.2 was set to 1.6*0.0237*0.07 ms^{-1} and is unregulated, reflecting constant exposure of the *Sphagnum* photosynthesising tissues to the atmosphere. The 1.6 is unitless and accounts for differing molecular diffusivity of CO_2 and water vapour in air, and 0.07 mol m^{-2}s^{-1} is the maximum CO_2 conductance measured in *Sphagnum* by Williams & Flanagan (1998). The value of 0.0237 m^{3}mol^{-1} is a fixed non-temperature-dependent amount for the molar volume. It is not clear that Williams & Flanagan's (1998) CO_2 conductance in mol m^{-2}s^{-1} within the living *Sphagnum* tissue would be constant with respect to temperature. Therefore, for simplicity, the molar conversion avoids temperature-dependence. This is in order to avoid adding complexity (adding temperature dependence to the *Sphagnum* volumetric gas absorption function) which may make the analysis of this initial model difficult. Williams & Flanagan (1998) ascribed lower values to desiccation-stress, which were not applied in our model because desiccation-stress is simulated independently using the desiccation stress factor, β, defined for our *Sphagnum* model in Table 2. This is based on field observations from Strack et al. (2009) (capitulum water content against WTP), Murray et al. (1989) and Riutta et al. (2007) (maximum *Sphagnum* photosynthetic production value occurs when the water table is just below the ground surface). It is also similar to the approach of Wania et al. (2009b), Yurova et al (2007) for their *Sphagnum* models. Only two simultaneous functions needed solving to simulate *Sphagnum* photosynthesis, represented by equations A.2 to A.5, leaving out completely the stomatal conductance term referred to in Table 2. Therefore, we changed the three-way simultaneous function described in appendix A.1 for vascular plants, to a two-way simultaneous function for non-vascular *Sphagnum*. The two unknown variables are A, and c_i. Combining equations A.1 and A.2 with equations A.3 (rubisco-limited net leaf photosynthesis), and then combining equations A.1 and A.2 with equation A.4 (light-limited net leaf photosynthesis), given that g_s is now fixed, gives equations A.12 and A.13:

$$0 = \frac{\alpha}{V_m} c_{ri}^2 + \left(\frac{\alpha}{V_m}(K - c_{atm}) - R_d + 1 \right) c_{ri} - \left(\frac{\alpha}{V_m} K c_{atm} + K R_d + \Gamma \right) \qquad \text{A.12}$$

$$0 = \frac{\alpha}{\gamma} c_{li}^2 + \left(\frac{\alpha}{\gamma}(2\Gamma - c_{atm}) - R_d + 1 \right) c_{li} - \left(\frac{\alpha}{V_m} K c_{atm} + K R_d + \Gamma \right) \qquad \text{A.13}$$

where $\alpha = \frac{g_s}{1.6RT^*\beta}$, $\gamma = 0.08(1 - \omega)I_{par}$, $K = K_c \left(1 + \frac{0_a}{K_0} \right)$. α, γ and K are terms to simplify equations A.17 and A.18.

In the new *Sphagnum* PFT, leaf-surface conductance is fixed and the rate of photosynthesis varies. Therefore, under different limited rates of photosynthesis, we have split c_i (internal leaf CO_2 partial pressure) to distinguish it between c_{ri} (under rubisco-limitation) and c_{li} (under light-limitation). In the equations for the prior vascular TRIFFID PFT, c_i was instead the same value under both limitations. (This does not affect the use of equations 1 and 2 to calculate g_s in the new *Sphagnum* PFT since these equations are not used to calculate g_s, which has a fixed value instead). The quadratic solutions to equations A.12 and A.13 give a positive and a negative value for c_{ri} and c_{li}. The positive solutions for c_{ri} and c_{li} were substituted respectively into equations A.3 and A.4 to give unique values of GPP_r and GPP_l. The question of whether to use the positive or negative quadratic solution was answered in the following way. The standard quadratic solution is:

$$c_i = \frac{-B \pm \sqrt{B^2 - 4AD}}{2A} \tag{A.14}$$

Applying equation A.14 to equations A.12 and A.13, where all the additional variables are positive numbers:

$$A_r = \left\{\frac{\alpha}{V_m}\right\}, A_l = \left\{\frac{\alpha}{\gamma}\right\} \tag{A.15}$$

It follows that $A > 0$ in both cases.

$$B_r = \frac{\alpha}{V_m}(K - c_{atm}) - R_d + 1, \qquad B_l = \frac{\alpha}{\gamma}(2\Gamma - c_{atm}) - R_d + 1 \tag{A.16}$$

It follows that $B > 0$ or $B < 0$ are both possible.

$$D_r = -\left\{\frac{\alpha}{V_m}Kc_{atm} + KR_d + \Gamma\right\}, \quad D_l = -\left\{\frac{\alpha}{\gamma}2\Gamma c_{atm} + 2\Gamma R_d + \Gamma\right\} \tag{A.17}$$

It follows that $D < 0$, therefore $-4AD > 0$, and $\sqrt{B^2 - 4AD} > B$. So in order for the quadratic equation to give positive values for c_{ri} and c_{li}, then its solution must take the form of equation A.18.

$$c_{ri}, c_{li} = \frac{-B + \sqrt{B^2 - 4AD}}{2A} \tag{A.18}$$

The smoothed minimum value for GPP is then calculated using the existing smoothing algorithm in TRIFFID (Clark et al. 2011) from the unique solutions to equations A.3 through A.5. This creates a new version of the photosynthesis process in Table 2 (Foley et al. 1996, Clark et al. 2011) adapted to accommodate the differences in the *Sphagnum* organism described in section 2.

Appendix B. Use of Shaping Parameters

B.1 Simulation of *Sphagnum* plant respiration

We compared the equations that simulate respiration in TRIFFID with the equivalent LPJ equations from Yurova et al. (2007), in order to correctly apply the *Sphagnum* field-derived parameterisations from LPJ's respiration

5 equations to TRIFFID.

In TRIFFID, R_p is a function of R_d, dark leaf respiration, in equations B.1 and B.7, which is simulated explicitly. Dark respiration is the plant respiration that occurs in cell mitochondria as opposed to photosynthesising cell components. The former provides energy for plant function whereas the latter reduces specifically photosynthetic

10 efficiency (Allaby, 2006).

Equations B.1 and B.6 have the same form, simulating R_p, in TRIFFID (R_{pT} - units of $kgCm^{-2}s^{-1}$) and LPJ-GUESS (R_{pLPJ} - units of $kgCm^{-2}d^{-1}$) respectively.

TRIFFID

15 $$R_{pT} = r_{gT}(\Pi_{GT} - R_{pmT}) + R_{pmT} \qquad \text{B.1}$$

$$\Pi_{GT} = 0.012(A_C + R_{dc}\beta) \qquad \text{B.2}$$

$$R_d = f_{dT} \cdot V_{max} f_T(2.0) \qquad \text{B.3}$$

$$R_{dc} = \sum(R_d) \qquad \text{B.4}$$

$$A_c = \sum(A) \qquad \text{B.5}$$

20

LPJ-GUESS

$$R_{pLPJ} = r_{gLPJ}(\Pi_{GLPJ} - R_{pnon-photLPJ} - R_{pphotLPJ}) + (R_{pnon-photLPJ} + R_{pphotLPJ}) \qquad \text{B.6}$$

R_{pmT} is plant maintenance respiration in TRIFFID; this is a function of canopy dark leaf respiration from equation

25 B.7 . The first right-hand term in equations B.1 and B.6 simulate growth respiration that is proportional to canopy

NPP, $(\prod_G - R_{pm})$ in TRIFFID, and $(\prod_G - R_{pnon-photLPJ} - R_{pphotLPJ})$ in LPJ. r_g is the growth respiration coefficient, and

$\prod_G$ is PFT-canopy GPP rate (kgC m^{-2}s^{-1}). The second right-hand terms simulate maintenance respiration. $R_{pnon\text{-}phot}$ and R_{pphot} in LPJ-GUESS refer to respiration in photosynthetic and non-photosynthetic tissues. R_{dc} and A_c, in TRIFFID, are canopy dark respiration and canopy net photosynthesis, upscaled from leaf dark respiration, R_d, and net leaf photosynthesis, A, using the 'big-leaf' method (see Clark et al. 2010; Clark et al. 2011; Cox, et al. 1999), in simplified equations B.4 and B.5. We used this method for simplicity and execution-speed; TRIFFID also has more sophisticated and less computationally efficient leaf-area upscaling methods that were not used. R_{pm} in TRIFFID is an equivalent term to ($R_{pnon\text{-}phot} + R_{pphot}$) in LPJ-GUESS.

TRIFFID

$$R_{pmT} = 0.012 \cdot R_{dc}\left\{\beta + \frac{N_r+N_s}{N_l}\right\} \tag{B.7}$$

N_l, is the leaf nitrogen content. N_s and N_r are the stem and root nitrogen contents. We split Equation B.7 to compare R_{pphotT} against $R_{pphotLPJ}$.

TRIFFID

$$R_{pmT} = R_{pnon-photT} + R_{pphotT} \tag{B.8}$$

$$R_{pphotT} = 0.0012 \cdot R_{dc} \cdot \beta \tag{B.9}$$

LPJ-GUESS

$$R_{pphotLPJ} = f_{dLPJ} \cdot V_{max} \tag{B.10}$$

Whereas in LPJ $R_{pphotLPJ}$ is non-temperature dependant (equation B.10), in TRIFFID R_{pphotT} has a Q10 temperature-dependence function (equations B.3, B.4, B.8 and B.9), but f_d, the unitless dark respiration scaling factor, in both LPJ and TRIFFID is applied simply to V_{max} (equations B.3 (TRIFFID) and B.10 (LPJ)), so the value $f_{dT} = f_{dLPJ} = 0.03$ for *Sphagnum* has been adopted for TRIFFID unchanged from LPJ.

29

Respiration within non-photosynthetic tissue again shows a similar form for LPJ-GUESS and TRIFFID.

TRIFFID

$$R_{pnon-photT} = 0.012 \cdot R_{dc} \left\{ \frac{N_r + N_s}{N_l} \right\} \qquad \qquad \textbf{B.11}$$

LPJ-GUESS

$$R_{pnon-photLPJ} = r_m \cdot k_r \cdot g(T_{air}) \left\{ \frac{M}{cn} \right\} \qquad \qquad \textbf{B.12}$$

In equation B.12 the combination of the shaping parameter r_m, k_r and $g(T_{air})$ represent a similar term to R_{dc} in TRIFFID. k_r (day^{-1}) is the respiration rate for a 10ºC baseline, and $g(T_{air})$ is a temperature response function (Yurova, et al. 2007). M is total biomass (kgCm^{-2}), cn is the C:N ratio. The term $\frac{M}{cn}$ represents the N content of the plant against the unitless mass-ratio term in TRIFFID of $\left\{ \frac{N_r + N_s}{N_l} \right\}$. The shaping parameterisation for $R_{pnon-photT}$ in TRIFFID comes again from the dark-respiration formulation in equation B.3, omitting the r_m shaping parameter from LPJ. The differing mass-ratios in these equations have not been reconciled between TRIFFID and LPJ-GUESS. Therefore the shaping parameter r_{gT} was calibrated in place of the two parameters r_{gLPJ} and r_{mLPJ} in LPJ-GUESS in order to fit the output curves in Figures 1 and 2. It is notable that r_{gT} with a value of 0.1 is lower than the similar r_{gLPJ} (0.5) or the value of r_{gT} previously used in TRIFFID, 0.25 (Clark et al. 2011) for vascular plants, and this implies that the values of f_{dT} and r_{gT} could be more tightly constrained, when more calibration data is available.

In summary, the value of f_d for TRIFFID in Table 4 has been established for *Sphagnum*, which is the same as the equivalent parameter in LPJ-GUESS. In this version of the TRIFFID *Sphagnum* model, parameter r_g is used as a shaping parameter.

B.2 *Sphagnum* Leaf Area Index

The model outputs did not fit the field-data of GPP against WTP from both Riutta et al (2007) and Strack et al (2009), without the LAI parameter being changed. Bond-Lamberty & Gower (2007) measured moss-LAI in a forested peatland, and found that *Sphagnum* and other boreal mosses have LAIs between 1 and 10. Glenn et al. (2006) measured the LAI of *Sphagnum* in a nutrient-poor fen as 1. Rydin et al (2006) noted that *Sphagnum* species

Geoscientific
Model Development
Discussions

that form lawns have lower shoot-density than those that form hummocks. The former include the species examined in Riutta et al (2007), the latter include the species in Strack et al (2009). Therefore LAI=1 (equivalent to lower shoot density) was applied to fit the model to data from Riutta et al (2007) (lawn/fen species with lower shoot-density) and this parameter was changed to LAI=3 (equivalent to higher shoot-density) in order to fit the data from

5   Strack et al (2009) (hummock/bog species with higher shoot-density). In addition, it is also plausible that a different desiccation stress function is required for these different *Sphagnum* species, with different parameters for the equation that defines β$_{Sphagnum}$ in Table 2, but different stress functions have not been developed here.

Code Availability

We have modified subroutines in the Surface section of the JULES v2.1 model code. This changed code is available

10   at the DOI link in Coppell (2019), for which we obtained permission from the Met Office. We must emphasise that JULES v2.1 is not the latest version of JULES and differs in much of its functionality from the latest version. Permission and license-information to use the whole JULES model is available from http://jules-lsm.github.io/access_req/JULES_access.html , from where the complete original JULES v2.1 model may be requested by email.

15   **Author Contribution**

Richard Coppell – developed the simultaneous-function part of the model with EG and designed and implemented all other parts of the model, tuned and tested, and co-wrote the paper with JH.
Emanuel Gloor – developed the simultaneous-function element of the model with RC and proof-read the paper.
Joseph Holden – supervised and co-wrote the paper with RC.

20   **Competing Interests**

The authors declare that they have no conflict of interest.

References

Allaby, M.: Oxford Dictionary of Plant Sciences, 2nd ed., Oxford University Press, Oxford, 2006.

Amthor, J. S., and Baldocchi, D. D.: Terrestrial Higher Plant Respiration and Net Primary Production. In Terrestrial Global Productivity, in: Terrestrial Global Productivity, edited by: Roy, J., Saugier, B., and Mooney, H. A.,
5   Academic Press Inc., San Diego, USA, 33-59, 2001.

Baird, A. J., Belyea, L. R., and Morris, P. J.: Upscaling of Peatland-Atmosphere Fluxes of Methane: Small-Scale Heterogeneity in Process Rates and the Pitfalls of "Bucket-and-Slab" Models, Carbon Cycling in Northern Peatlands, 184, 37-53, 10.1029/2008gm000826, 2009.

10

Begon, M., Townsend, C. R., and Harper, J. L.: Ecology From Individuals to Ecosystems, 4th ed., Wiley-Blackwell, Malden, MA ; Oxford, 2006.

Belyea, L. R., and Baird, A. J.: Beyond "The limits to peat bog growth": Cross-scale feedback in peatland
15   development, Ecological Monographs, 76, 299-322, 10.1890/0012-9615(2006)076[0299:btltpb]2.0.co;2, 2006a.

Belyea, L. R., and Baird, A. J.: Beyond "The limits to peat bog growth": Cross-scale feedback in peatland development, Ecological Monographs, 76, 299-322, 10.1890/0012-9615(2006)076[0299:btltpb]2.0.co;2, 2006b.

20   Belyea, L. R.: Nonlinear Dynamics of Peatlands and Potential Feedbacks on the Climate System, Carbon Cycling in Northern Peatlands, 184, 5-18, 10.1029/2008gm000829, 2009.

Beringer, J., Lynch, A. H., Chapin, F. S., Mack, M., and Bonan, G. B.: The representation of arctic soils in the land surface model: The importance of mosses, Journal of Climate, 14, 3324-3335, 10.1175/1520-
25   0442(2001)014<3324:troasi>2.0.co;2, 2001.

Best, M. J., Pryor, M., Clark, D. B., Rooney, G. G., Essery, R. L. H., Menard, C. B., Edwards, J. M., Hendry, M. A., Porson, A., Gedney, N., Mercado, L. M., Sitch, S., Blyth, E., Boucher, O., Cox, P. M., Grimmond, C. S. B.,

and Harding, R. J.: The Joint UK Land Environment Simulator (JULES), model description - Part 1: Energy and water fluxes, Geoscientific Model Development, 4, 677-699, 10.5194/gmd-4-677-2011, 2011.

Beven, K.: Causal models as multiple working hypotheses about environmental processes, Comptes Rendus
5 Geoscience, 344, 77-88, 10.1016/j.crte.2012.01.005, 2012.

Bewley, J. D., Halmer, P., Krochko, J., and Winner, W. E.: Metabolism of a drought-tolerant and a drought-sensitive moss: respiration, ATP synthesis and carbohydrate status, in: Dry Biological Systems, edited by: Crowe, J. H., and Clegg, J. S., Academic Press, Inc., New York, 185-205, 1978.
10

Bond-Lamberty, B., Wang, C. K., and Gower, S. T.: Net primary production and net ecosystem production of a boreal black spruce wildfire chronosequence, Global Change Biology, 10, 473-487, 10.1111/j.1529-8817.2003.0742.x, 2004.

15 Bragg, O., and Lindsay, R.: Strategy and Action Plan for Mire and Peatland Conservation in Central Europe, Wageningen, The Netherlands, 94 pp., 2003.

Brovkin, V., Ganopolski, A., and Svirezhev, Y.: A continuous climate-vegetation classification for use in climate-biosphere studies, Ecological Modelling, 101, 251-261, 10.1016/s0304-3800(97)00049-5, 1997.
20

Bu, Z. J., Zheng, X. X., Rydin, H., Moore, T., and Ma, J. Z.: Facilitation vs. competition: Does interspecific interaction affect drought responses in *Sphagnum*?, Basic and Applied Ecology, 14, 574-584, 10.1016/j.baae.2013.08.002, 2013.

25 Carleton, T. J., and Dunham, K. M. M.: Distillation in a boreal mossy forest floor, Canadian Journal of Forest Research-Revue Canadienne De Recherche Forestiere, 33, 663-671, 10.1139/x02-197, 2003.

Charman, D.: Peatlands and Environmental Change, Wiley, Chichester, UK, 301 pp., 2002.

Charman, D. J., Beilman, D. W., Blaauw, M., Booth, R. K., Brewer, S., Chambers, F. M., Christen, J. A., Gallego-Sala, A., Harrison, S. P., Hughes, P. D. M., Jackson, S. T., Korhola, A., Mauquoy, D., Mitchell, F. J. G., Prentice, I. C., van der Linden, M., De Vleeschouwer, F., Yu, Z. C., Alm, J., Bauer, I. E., Corish, Y. M. C., Garneau, M., Hohl, V., Huang, Y., Karofeld, E., Le Roux, G., Loisel, J., Moschen, R., Nichols, J. E., Nieminen, T. M., MacDonald, G. M., Phadtare, N. R., Rausch, N., Sillasoo, U., Swindles, G. T., Tuittila, E. S., Ukonmaanaho, L., Valiranta, M., van Bellen, S., van Geel, B., Vitt, D. H., and Zhao, Y.: Climate-related changes in peatland carbon accumulation during the last millennium, Biogeosciences, 10, 929-944, 10.5194/bg-10-929-2013, 2013.

Clark, D., Harris, P., Pryor, M., and Hendry, M.: Joint UK Land Environment Simulator (JULES) Version 2.2 User Manual. The Centre for Ecology & Hydrology, UK. Hadley Centre for Climate Prediction and Research, UK., Wallingford, Oxfordhire, UK, 2010.

Clark, D. B., and Gedney, N.: Representing the effects of subgrid variability of soil moisture on runoff generation in a land surface model, Journal of Geophysical Research-Atmospheres, 113, 10.1029/2007jd008940, 2008.

Clark, D. B., Mercado, L. M., Sitch, S., Jones, C. D., Gedney, N., Best, M. J., Pryor, M., Rooney, G. G., Essery, R. L. H., Blyth, E., Boucher, O., Harding, R. J., Huntingford, C., and Cox, P. M.: The Joint UK Land Environment Simulator (JULES), model description - Part 2: Carbon fluxes and vegetation dynamics, Geoscientific Model Development, 4, 701-722, 10.5194/gmd-4-701-2011, 2011.

Clymo, R. S., and Hayward, P. M.: The Ecology of *Sphagnum*, in: Bryophyte Ecology, edited by: Smith, A. I. E., Springer, Netherlands, 229-289, 1982.

Coppell, R.: JULES DGVM modified SURFACE subroutines only, incorporating Sphagnum PFT func. University of Leeds. [Dataset]. https://doi.org/10.5518/567, 2019.

Cox, P. M., Huntingford, C., and Harding, R. J.: A canopy conductance and photosynthesis model for use in a GCM land surface scheme, Journal of Hydrology, 212, 79-94, 10.1016/s0022-1694(98)00203-0, 1998.

Cox, P. M., Betts, R. A., Bunton, C. B., Essery, R. L. H., Rowntree, P. R., and Smith, J.: The impact of new land surface physics on the GCM simulation of climate and climate sensitivity, Climate Dynamics, 15, 183-203, 10.1007/s003820050276, 1999.

5   Cox, P. M., Betts, R. A., Jones, C. D., Spall, S. A., and Totterdell, I.: Modelling vegetation and the carbon cycle as interactive elements of the climate system. In: Hadley Centre Technical Notes, 2001.

Dimitrov, D. D., Grant, R. F., Lafleur, P. M., and Humphreys, E. R.: Modeling the effects of hydrology on gross primary productivity and net ecosystem productivity at Mer Bleue bog, Journal of Geophysical Research-Biogeosciences, 116, 10.1029/2010jg001586, 2011.

10

Druel, A., Peylin, P., Krinner, G., Ciais, P., Viovy, N., Peregon, A., Bastrikov, V., Kosykh, N., and Mironycheva-Tokareva, N.: Towards a more detailed representation of high-latitude vegetation in the global land surface model ORCHIDEE (ORC-HL-VEGv1.0), Geoscientific Model Development, 10, 4693-4722, 10.5194/gmd-10-4693-2017, 2017.

15

Euskirchen, E. S., McGuire, A. D., Chapin, F. S., Yi, S., and Thompson, C. C.: Changes in vegetation in northern Alaska under scenarios of climate change, 2003-2100: implications for climate feedbacks, Ecological Applications, 19, 1022-1043, 10.1890/08-0806.1, 2009.

20

Foley, J. A., Prentice, I. C., Ramankutty, N., Levis, S., Pollard, D., Sitch, S., and Haxeltine, A.: An integrated biosphere model of land surface processes, terrestrial carbon balance, and vegetation dynamics, Global Biogeochemical Cycles, 10, 603-628, 10.1029/96gb02692, 1996.

25   Frolking, S., Roulet, N. T., Moore, T. R., Richard, P. J. H., Lavoie, M., and Muller, S. D.: Modeling northern peatland decomposition and peat accumulation, Ecosystems, 4, 479-498, 10.1007/s10021-001-0105-1, 2001.

Frolking , S., Roulet , N., and Lawrence, D.: Issues related to incorporating northern peatlands into Global Climate Models., in: Carbon cycling in northern peatlands. American Geophysical Union Monograph, edited by: Baird AJ, B. L., Comas X, Reeve AS, Slater LD, 184, American Geophysical Union, Washington DC, 19-36, 2009.

5   Gao, Q., Yu, M., and Zhou, C.: Detecting the Differences in Responses of Stomatal Conductance to Moisture Stresses between Deciduous Shrubs and Artemisia Subshrubs, PlosOne, 8, e84200, 10.1371/journal.pone.0084200, 2013.

Gerdol, R., Bonora, A., Marchesini, R., Gualandri, R., and Pancaldi, S.: Growth response of *Sphagnum*
10   capillifolium to nighttime temperature and nutrient level: Mechanisms and implications for global change, Arctic and Alpine Research, 30, 388-395, 10.2307/1552011, 1998.

Glenn, A. J., Flanagan, L. B., Syed, K. H., and Carlson, P. J.: Comparison of net ecosystem CO_2 exchange in two peatlands in western Canada with contrasting dominant vegetation, *Sphagnum* and Carex, Agricultural and Forest
15   Meteorology, 140, 115-135, 10.1016/j.agrformet.2006.03.020, 2006.

Hajek, T., and Beckett, R. P.: Effect of water content components on desiccation and recovery in *Sphagnum* mosses, Annals of Botany, 101, 165-173, 10.1093/aob/mcm287, 2008.

20   Hajek, T., Ballance, S., Limpens, J., Zijlstra, M., and Verhoeven, J. T. A.: Cell-wall polysaccharides play an important role in decay resistance of *Sphagnum* and actively depressed decomposition in vitro, Biogeochemistry, 103, 45-57, 10.1007/s10533-010-9444-3, 2011.

Harper, A.B., Wiltshire, A.J., Cox, P.M., Friedlingstein, P., Jones, C.D., Mercado, L.M., Sitch, S., Williams, K.,
25   Duran-Rojas, C., 2018. Vegetation distribution and terrestrial carbon cycle in a carbon cycle configuration of JULES4.6 with new plant functional types. Geoscientific Model Development 11, 2857-2873.

Haxeltine, A., and Prentice, I. C.: BIOME3: An equilibrium terrestrial biosphere model based on ecophysiological constraints, resource availability, and competition among plant functional types, Global Biogeochemical Cycles, 10, 693-709, 10.1029/96gb02344, 1996.

5   Hayman, G. D., O'Connor, F. M., Dalvi, M., Clark, D. B., Gedney, N., Huntingford, C., Prigent, C., Buchwitz, M., Schneising, O., Burrows, J. P., Wilson, C., Richards, N., and Chipperfield, N.: Comparison of the HadGEM2 climate-chemistry model against in-situ and SCIAMACHY atmospheric methane data, Atmos. Chem. Phys. Discuss., 14, 12967-13020, 10.5194/acpd-14-12967-2014, 2014.

10 Hayward, P. M., and Clymo, R. S.: Profiles of water-content and pore-size in *Sphagnum* and peat, and their relation to peat bog ecology, Proceedings of the Royal Society Series B-Biological Sciences, 215, 299-325, 10.1098/rspb.1982.0044, 1982.

Hughes, J. K., Valdes, P. J., and Betts, R. A.: Dynamical properties of the TRIFFID dynamic global vegetation
15 model. In: Hadley Centre Technical Notes, 56, 2004.

Jobbagy, E. G., and Jackson, R. B.: The vertical distribution of soil organic carbon and its relation to climate and vegetation, Ecological Applications, 10, 423-436, 10.2307/2641104, 2000.

20 Johnson, M. G., Granath, G., Tahvanainen, T., Pouliot, R., Stenoien, H. K., Rochefort, L., Rydin, H., and Shaw, A. J.: Evolution of niche preference in *Sphagnum* peat mosses, Evolution, 69, 90-103, 10.1111/evo.12547, 2015.

Kangas, L., Maanavilja, L., Hajek, T., Juurola, E., Chimner, R. A., Mehtatalo, L., and Tuittila, E. S.: Photosynthetic traits of *Sphagnum* and feather moss species in undrained, drained and rewetted boreal spruce swamp forests,
25 Ecology and Evolution, 4, 381-396, 10.1002/ece3.939, 2014.

Lamers, L. P. M., Farhoush, C., Van Groenendael, J. M., and Roelofs, J. G. M.: Calcareous groundwater raises bogs; the concept of ombrotrophy revisited, Journal of Ecology, 87, 639-648, 10.1046/j.1365-2745.1999.00380.x, 1999.

Laurent, J. M., Bar-Hen, A., Francois, L., Ghislain, M., and Cheddadi, R.: Refining vegetation simulation models: From plant functional types to bioclimatic affinity groups of plants, Journal of Vegetation Science, 15, 739-746, 10.1111/j.1654-1103.2004.tb02316.x, 2004.

5

Leuning, R.: A critical-appraisal of a combined stomatal-photosynthesis model for C-3 plants, Plant Cell and Environment, 18, 339-355, 10.1111/j.1365-3040.1995.tb00370.x, 1995.

Limpens, J., Berendse, F., Blodau, C., Canadell, J. G., Freeman, C., Holden, J., Roulet, N., Rydin, H., and
10   Schaepman-Strub, G.: Peatlands and the carbon cycle: from local processes to global implications - a synthesis, Biogeosciences, 5, 1475-1491, 2008.

Lindo, Z., and Gonzalez, A.: The Bryosphere: An Integral and Influential Component of the Earth's Biosphere, Ecosystems, 13, 612-627, 10.1007/s10021-010-9336-3, 2010.

15

Loisel, J., Garneau, M., and Helie, J. F.: Modern *Sphagnum* delta C-13 signatures follow a surface moisture gradient in two boreal peat bogs, James Bay lowlands, Quebec, Journal of Quaternary Science, 24, 209-214, 10.1002/jqs.1221, 2009.

20   Loisel, J., Gallego-Sala, A. V., and Yu, Z.: Global-scale pattern of peatland *Sphagnum* growth driven by photosynthetically active radiation and growing season length, Biogeosciences, 9, 2737-2746, 10.5194/bg-9-2737-2012, 2012.

Murray, K. J., Harley, P. C., Beyers, J., Walz, H., and Tenhunen, J. D.: Water-content effects on photosynthetic
25   response of *Sphagnum* mosses from the foothills of the Philip Smith Mountains, Alaska, Oecologia, 79, 244-250, 10.1007/bf00388484, 1989.

O'Connor, F. M., Boucher, O., Gedney, N., Jones, C. D., Folberth, G. A., Coppell, R., Friedlingstein, P., Collins, W. J., Chappellaz, J., Ridley, J., and Johnson, C. E.: Possible role of wetlands, permafrost, and methane hydrates

in the methane cycle under future climate change: a review, Reviews of Geophysics, 48, 10.1029/2010rg000326, 2010.

Pope, V. D., Gallani, M. L., Rowntree, P. R., and Stratton, R. A.: The impact of new physical parametrizations in the Hadley Centre climate model: HadAM3, Climate Dynamics, 16, 123-146, 10.1007/s003820050009, 2000.

Prentice, I. C., Cramer, W., Harrison, S. P., Leemans, R., Monserud, R. A., and Solomon, A. M.: A global biome model based on plant physiology and dominance, soil properties and climate., Journal of Biogeography, 19, 117-134, 10.2307/2845499, 1992.

Price, G. D., McKenzie, J. E., Pilcher, J. R., and Hoper, S. T.: Carbon-isotope variation in *Sphagnum* form hummock-hollow complexes: Implications for Holocene climate reconstruction, Holocene, 7, 229-233, 10.1177/095968369700700211, 1997.

Proctor, M. C. F., Raven, J. A., and Rice, S. K.: Stable carbon isotope discrimination measurements in *Sphagnum* and other bryophytes - physiological and ecological implications, Journal of Bryology, 17, 193-202, 1992.

Qiu, C. J., Zhu, D., Ciais, P., Guenet, B., Krinner, G., Peng, S. S., Aurela, M., Bernhofer, C., Brummer, C., Bret-Harte, S., Chu, H. S., Chen, J. Q., Desai, A. R., Dusek, J., Euskirchen, E. S., Fortuniak, K., Flanagan, L. B., Friborg, T., Grygoruk, M., Gogo, S., Grunwald, T., Hansen, B. U., Holl, D., Humphreys, E., Hurkuck, M., Kiely, G., Klatt, J., Kutzbach, L., Largeron, C., Laggoun-Defarge, F., Lund, M., Lafleur, P. M., Li, X. F., Mammarella, I., Merbold, L., Nilsson, M. B., Olejnik, J., Ottosson-Lofvenius, M., Oechel, W., Parmentier, F. J. W., Peichl, M., Pirk, N., Peltola, O., Pawlak, W., Rasse, D., Rinne, J., Shaver, G., Schmid, H. P., Sottocornola, M., Steinbrecher, R., Sachs, T., Urbaniak, M., Zona, D., and Ziemblinska, K.: ORCHIDEE-PEAT (revision 4596), a model for northern peatland CO_2, water, and energy fluxes on daily to annual scales, Geoscientific Model Development, 11, 497-519, 10.5194/gmd-11-497-2018, 2018.

Randall, D. A., Dazlich, D. A., Zhang, C., Denning, A. S., Sellers, P. J., Tucker, C. J., Bounoua, L., Los, S. O., Justice, C. O., and Fung, I.: A revised land surface parameterization (SiB2) for GCMs .3. The greening of the

Colorado State University general circulation model, Journal of Climate, 9, 738-763, 10.1175/1520-0442(1996)009<0738:arlspf>2.0.co;2, 1996.

Rice, S. K.: Variation in carbon isotope discrimination within and among *Sphagnum* species in a temperate wetland,
5   Oecologia, 123, 1-8, 10.1007/s004420050983, 2000.

Riutta, T., Laine, J., and Tuittila, E. S.: Sensitivity of CO_2 exchange of fen ecosystem components to water level variation, Ecosystems, 10, 718-733, 10.1007/s10021-007-9046-7, 2007.

10   Rydin, H.: Effect of water level on desiccation of *Sphagnum* in relation to surrounding *Sphagna*, Oikos, 45, 374-379, 10.2307/3565573, 1985.

Rydin, H.: Competition and niche separation in *Sphagnum*, Canadian Journal of Botany-Revue Canadienne De Botanique, 64, 1817-1824, 1986.
15

Rydin , H., Gunnarsson , U., and Sundberg , S.: The Role of *Sphagnum* in Peatland Development and Persistence., in: Boreal Peatland Ecosystems, edited by: Wieder , R. K., Vitt , D.H., Springer- Verlag, Berlin, 47-65, 2006.

Rydin, H., and Jeglum, J. K.: The biology of peatlands, Oxford University Press, Oxford, 1 pp., 2006.
20

Sellers, P. J., Los, S. O., Tucker, C. J., Justice, C. O., Dazlich, D. A., Collatz, G. J., and Randall, D. A.: A revised land surface parameterization (SiB2) for atmospheric GCMs .2. The generation of global fields of terrestrial biophysical parameters from satellite data, Journal of Climate, 9, 706-737, 10.1175/1520-0442(1996)009<0706:arlspf>2.0.co;2, 1996a.
25

Sellers, P. J., Randall, D. A., Collatz, G. J., Berry, J. A., Field, C. B., Dazlich, D. A., Zhang, C., Collelo, G. D., and Bounoua, L.: A revised land surface parameterization (SiB2) for atmospheric GCMs .1. Model formulation, Journal of Climate, 9, 676-705, 10.1175/1520-0442(1996)009<0676:arlspf>2.0.co;2, 1996b.

Sitch, S., Smith, B., Prentice, I. C., Arneth, A., Bondeau, A., Cramer, W., Kaplan, J. O., Levis, S., Lucht, W., Sykes, M. T., Thonicke, K., and Venevsky, S.: Evaluation of ecosystem dynamics, plant geography and terrestrial carbon cycling in the LPJ dynamic global vegetation model, Global Change Biology, 9, 161-185, 10.1046/j.1365-2486.2003.00569.x, 2003.

5

Skre, O., and Oechel, W. C.: Moss functioning in different taiga ecosystems in interior Alaska .1. Seasonal, phenotypic, and drought effects on photosynthesis and response patterns, Oecologia, 48, 50-59, 10.1007/bf00346987, 1981.

10   Smolders, A. J. P., Tomassen, H. B. M., Pijnappel, H. W., Lamers, L. P. M., and Roelofs, J. G. M.: Substrate-derived CO_2 is important in the development of *Sphagnum* spp, New Phytologist, 152, 325-332, 10.1046/j.0028-646X.2001.00261.x, 2001.

Sonnentag, O., Chen, J. M., Roulet, N. T., Ju, W., and Govind, A.: Spatially explicit simulation of peatland
15   hydrology and carbon dioxide exchange: Influence of mesoscale topography, Journal of Geophysical Research-Biogeosciences, 113, 10.1029/2007jg000605, 2008.

Strack, M., Waddington, J. M., Lucchese, M. C., and Cagampan, J. P.: Moisture controls on CO_2 exchange in a *Sphagnum*-dominated peatland: results from an extreme drought field experiment, Ecohydrology, 2, 454-461,
20   10.1002/eco.68, 2009.

Street, L. E., Subke, J.-A., Sommerkorn, M., Sloan, V., Ducrotoy, H., Phoenix, G. K., and Williams, M.: The role of mosses in carbon uptake and partitioning in arctic vegetation, New Phytologist, 199, 163-175, 10.1111/nph.12285, 2013.

25

Thompson, D. K., and Waddington, J. M.: *Sphagnum* under pressure: towards an ecohydrological approach to examining *Sphagnum* productivity, Ecohydrology, 1, 299-308, 10.1002/eco.31, 2008.

Vanbreemen, N.: HOW *SPHAGNUM* BOGS DOWN OTHER PLANTS, Trends in Ecology & Evolution, 10, 270-275, 10.1016/0169-5347(95)90007-1, 1995.

Waddington, J. M., and Roulet, N. T.: Atmosphere-wetland carbon exchanges: Scale dependency of CO_2 and CH_4
5   exchange on the developmental topography of a peatland, Global Biogeochemical Cycles, 10, 233-245, 10.1029/95gb03871, 1996.

Wania, R., Ross, I., and Prentice, I. C.: Integrating peatlands and permafrost into a dynamic global vegetation model: 1. Evaluation and sensitivity of physical land surface processes, Global Biogeochemical Cycles, 23,
10   10.1029/2008gb003412, 2009a.

Wania, R., Ross, I., and Prentice, I. C.: Integrating peatlands and permafrost into a dynamic global vegetation model: 2. Evaluation and sensitivity of vegetation and carbon cycle processes, Global Biogeochemical Cycles, 23, 15, 10.1029/2008gb003413, 2009b.

15

Wieder, R. K.: Primary production in boreal peatlands, Ecological Studies, 188, 145-164, 2006.

Williams, T. G., and Flanagan, L. B.: Measuring and modelling environmental influences on photosynthetic gas exchange in *Sphagnum* and Pleurozium, Plant Cell and Environment, 21, 555-564, 10.1046/j.1365-
20   3040.1998.00292.x, 1998.

Woodward, F. I.: Predictions and measurements of the maximum photosynthetic rate, Amax, at the global scale., in: Ecophysiology: photosynthesis, edited by: Schulze, E. D., and Caldwell, M. M., Springer-Verlag, Berlin, 491-509, 1994.

25

Yu, Z. C., Loisel, J., Brosseau, D. P., Beilman, D. W., and Hunt, S. J.: Global peatland dynamics since the Last Glacial Maximum, Geophysical Research Letters, 37, 10.1029/2010gl043584, 2010.

Yu, Z. C.: Holocene carbon flux histories of the world's peatlands: Global carbon-cycle implications, Holocene, 21, 761-774, 10.1177/0959683610386982, 2011.

Yurova, A., Wolf, A., Sagerfors, J., and Nilsson, M.: Variations in net ecosystem exchange of carbon dioxide in a boreal mire: Modeling mechanisms linked to water table position, Journal of Geophysical Research-Biogeosciences, 112, 10.1029/2006jg000342, 2007.